Using Topology Optimization to Numerically Improve Barriers to Reverse Engineering

Devin D. LeBaron
Research Assistant
e-mail: dblebaron@gmail.com

Christopher A. Mattson[1]
Associate Professor
e-mail: mattson@byu.edu

Department of Mechanical Engineering,
Brigham Young University,
Provo, UT 84602

Here explored is a method by which designers can use the tool of topology optimization to numerically improve barriers to reverse engineering. Recently developed metrics, which characterize the time (T) to reverse engineer a product, enable this optimization. A key parameter used in the calculation of T is information content *(K). The method presented in this paper pursues traditional topology optimization objectives while simultaneously maximizing K, and thus T, in the resulting topology. New aspects of this paper include algorithms to (1) evaluate K for any topology, (2) increase K for a topology by manipulating macroscale geometry* and *microscale crystallographic information for each element, and (3) simultaneously maximize K and minimize structural compliance (a traditional topology optimization objective). These algorithms lead designers to desirable topologies with increased barriers to reverse engineering. The authors conclude that barriers to reverse engineering can indeed be increased without sacrificing the desirable structural characteristic of compliance. This has been shown through the example of a novel electrical contact for a consumer electronics product.* [DOI: 10.1115/1.4025962]

1 Introduction and Background

Innovative products are reverse engineered—often by competitors seeking to capture market share. The share gained is directly related to the time it takes to enter the market [1]. Therefore, it is beneficial for innovating companies to impede the reverse engineering efforts of others. This paper shows that incorporating macro and microscale barriers within products will increase the time required to reverse engineer them, presumably delaying competitors' market entry.

Various ways to impede reverse engineering have been explored. Methods include: avoiding explicit disclosure of information [2], creating antirobust designs [2,3], designing components that are difficult to access [4], designing components that require unique tools or information [4,5], and designing components that self destruct when tampered with [4]. Others have explored ways to use existing design methods such as TRIZ [6]. In this paper, we explore the use of topology optimization to impede reverse engineering.

Metrics to define and evaluate barriers to reverse engineering have recently been developed [7,8]. The ability to quantify these barriers enables their implementation into topology optimization and other numerical optimization frameworks. We briefly review the definitions and metrics created for barriers to reverse engineering and highlight how they can be used in protecting innovative products.

A barrier to reverse engineering has been defined as anything that impedes the extraction of information about a product from the product itself [7]. The metrics are summarized below in the equations for B, the barrier to reverse engineering, and T, the time to reverse engineer a product [8].

$$B = P/F^2 \tag{1}$$

$$T = -BS\ln(K/K_0) \tag{2}$$

where P is the power (work per time to extract information), F is the rate of information extraction, K is the information content, and S is the information storage capacity. B and T are related but distinct as described in Harston and Mattson [8]. Often the goal in creating barriers to reverse engineering is to delay the competition until the market is saturated [9]. Thus, we will focus on the maximization of T. Increasing T can be accomplished through increasing B, S, and/or K. Within a topology optimization framework, the information content (K) is related only to the product itself and not to the individual who is reverse engineering it (as is the case for B and S). Therefore, K is generally evaluated and can be automatically extracted for any generated topology. In this paper, we indirectly maximize T by maximizing K.

Before presenting our approach for simultaneously optimizing topology and reverse engineering objectives, we must first provide a brief description of two supporting technologies; topology optimization and microstructure sensitive design.

Topology optimization is a design tool that distributes material in an optimal lay-out within a design domain. Topology optimization's most common use is for the optimal lay-out of isotropic material in linear-elastic structural problems. In this scenario, the known values are the loads, support conditions, and volume of the structure [10]. Although structural applications of this design tool are the most common, it has been used to optimize performance in a variety of other categories such as, thermal expansion [11], compliant mechanisms [12,13], piezoelectric surfaces [14], electromagnetic properties [15], material selection [16], and heat transfer [17,18], to name a few. To the author's best knowledge, topology optimization has not yet been described in the literature as a means to impede reverse engineering. This paper uses topology optimization to optimize structural characteristics as well as barriers to reverse engineering.

There is a variety of methods that have been developed to perform topology optimization. The most common is the solid isotropic material with penalization (SIMP) method. This method was first proposed in 1989 by Bendsoe [19]. With a few exceptions, all the commercial topology optimization software packages use this method [20]. Other methods that have been developed include the Evolutionary Structural Optimization (ESO) method, the Bi-directional Evolutionary Structural Optimization (BESO) method, derivative based methods and level-set methods. The SIMP method and the level-set method will be discussed further in this paper.

The SIMP method is also referred to as the "power-law approach." In this method, the design domain is discretized with elements having constant material properties. Each element also is

[1]Corresponding author.

Contributed by the Design Automation Committee of ASME for publication in the Journal of Mechanical Design. Manuscript received February 26, 2013; final manuscript received October 19, 2013; published online December 11, 2013. Assoc. Editor: Shinji Nishiwaki.

given a relative density value. These relative density values become the variables in the optimization problem. Each element's material properties become defined as the relative density raised to some power times the material property [21]. This is a finite element based method and has been used in many applications. This approach also requires filtering techniques to ensure that a solution is found. Hundreds of papers have been written on the SIMP method and varieties of the SIMP method. This paper uses the SIMP method in conjunction with other algorithms to complete its objectives.

More recently, level-set methods of Topology optimization have been developed [22,23]. These methods allow the designer to select the number of voids initially in the design domain. This would be useful for our application because (as described in Sec. 2.3) our method artificially introduces voids within the design domain as a means to increase information content. Level-set methods were not used in this paper because the SIMP method gives more control of the location of the introduced voids. However, implementation of the level-set method in the future could prove more effective in increasing barriers to reverse engineering.

Microstructure sensitive design is the process of establishing location and orientation of microstructure types within a part or component to attain desired performance [24]. Material microstructure refers to the organization of the crystalline grain structures in a material. For anisotropic materials, the microstructure is such that the material properties vary in different directions. In this paper, microstructure sensitive design is used to orient individual anisotropic elements in a topology to change its overall compliance. We recognize that there are no common manufacturing practices to manipulate the microstructure of each element individually—although previous work has suggested some ideas to accomplish this [25]. The present paper focuses on the theories of impeding reverse engineering and not necessarily on manufacturing feasibility.

For clarity, this paper does not offer contributions to the fields of topology optimization nor microstructure sensitive design; rather its new aspects offer contributions to the field of impeding reverse engineering. Namely this paper introduces algorithms to (1) evaluate K for any topology, (2) increase K for a topology by manipulating macroscale geometry *and* microstructure for each element, and (3) simultaneously maximize K and minimize structural compliance.

The remainder of this paper is outlined as follows: In Sec. 2, algorithms developed to evaluate and increase information content (K) within a topology are presented. In Sec. 3, an example of information content (K) being increased using topology optimization is shown through the design of a novel electrical contact for a consumer electronics product. In Sec. 4, our conclusions are presented.

2 New Developments for Increasing Barriers to Reverse Engineering

In this section, we present new developments that enable topology optimization to be used to numerically increase barriers to reverse engineering. An optimization problem formulation is provided, and a means to quantify the information content and maximize it—for any topology— is presented.

2.1 Optimization Problem Formulation In order to maximize information content while minimizing compliance we use the following multi-objective problem formulation:

$$\min_x J(x) = C(x) - Km(x) - Kg(x) \tag{3}$$

subject to

$$V_x/V_0 = v \tag{4}$$

$$ku = f \tag{5}$$

$$0 < x_{\min} \le x \le 1 \tag{6}$$

$$0 \le \Theta \le 360 \tag{7}$$

where C is the structural compliance; K_m is the information content in the microstructure; K_g is the information content in the geometry; x is a vector of element densities; $x_{\min}$ is a vector of minimum densities for the structural elements; k, u, and f are the stiffness matrix, displacement vectors, and force vectors, respectively; V_x and V_0 are the material volume and design domain volume; v is the volume fraction; and Θ is the microstructure orientation of each element. Additional constraints related to C are discussed in Sigmund et al [21].

There are two approaches to solve this problem, or any multi-objective optimization problem. The first is integrated generating and choosing [26]. The second is generate first, choose later [27]. We use the integrated generating and choosing for the remainder of this paper—of the form

$$J(x) = w_1 C(x) - w_2 Km(x) - w_3 Kg(x) \tag{8}$$

w_1, w_2, and w_3 are designer defined weights that allow a preference in the resulting topology. We recognize the well-known deficiencies of weighted sum methods for use in multi-objective optimization problems. Specifically, their inability to find solutions in nonconvex regions of the design objective space. We note that any multi-objective algorithm can be chosen at the designers discretion. Algorithms include: the weighted square sum method, the compromise programming method, or the physical programming method. We have chosen to use the simple weighted sum method here because it worked well for the examples in this paper and is conceptually simple and briefly describable.

2.1.1 Topology Optimization Set Up. A modified version of the 99-line topology optimization code developed by Sigmund et al [21] is used in this paper. This code allows the designer to define a two-dimensional design domain with boundary conditions and loads. Its objective is to minimize compliance for a given volume fraction. For full details on this code, the reader is referred to Sigmund et al [21]. Although this code is currently for two-dimensional problems it can be extended to three dimensions [21]. This extension can also be made to the algorithms presented in this paper. The design domain of the examples presented in this section is constrained to half of the MBB-beam as shown in Fig. 1, and the dimensions are 60 units in the horizontal direction, 30 in the vertical direction, and the volume fraction is 0.5.

When comparing topology optimization results in this paper, the variables $\bar{C}_i$ and $\bar{K}_i$ will be used. These variables are the average elemental compliance (C) and information content (K)

Fig. 1 Design domain used for all the examples in Sec. 2. Dimensions are 60 units in the horizontal direction and 30 units in the vertical direction. The design domain corresponds to half the MBB-beam.

normalized with respect to a benchmark design. The subscript i refers to which benchmark the topology is being compared to. The equations for $\bar{C}_i$ and $\bar{K}_i$ are shown as

$$\bar{C}_i = \left(\frac{C}{C_i} * 100\right) \tag{9}$$

$$\bar{K}_i = \left(\frac{K}{K_i} * 100\right) \tag{10}$$

where C and K are evaluated for the current topology, and C_i and K_i represent the C and K of the benchmark topology.

2.2 Quantification of Information Content (K). The information content in a product is the collection of information from different categories such as material, geometry, microstructure, electrical conductivity, color, and other types of information [8]. This paper focuses only on increasing the information content in the geometry (Kg) and microstructure (Km) categories. To accomplish this, the information content must first be quantified. For geometry, the quantity of information content is the amount of data required to define the geometry. For microstructure, it is the number of distinct microstructures in a given topology. In this section, we describe the algorithm, we have developed to quantify the information content (K) in any topology.

Although it may seem simple to reverse engineer the geometry (as it is compared to the complexity of reverse engineering material microstructure) many papers in the literature express that reverse engineering geometry is not as simple as it seems [28–30] Additionally, our own experience is consistent with that in the literature.

To determine the geometric information content in a topology, the geometry is first decomposed into smaller constructs. To do so, all boundaries between material and the void (empty) regions in the design domain must be geometrically articulated. These boundaries can be represented by polygons as seen in Fig. 2. Each vertex of a polygon requires 2 data to be defined in a two dimensional setting. As the geometry is fully described by these polygons, two times the quantity of polygons' vertices is the quantity of data required to reproduce the topology.

Although quantifying the geometric information content in a topology can easily be done manually, the task needs to be automated to avoid interrupting the optimization routine at each topological iteration. In order to automate this process, Matlab's digital image processing function *convex hull* is used. The *convex hull* function is able to represent the void regions in the design domain as polygons. These polygons are then used to calculate the amount of geometric information content as described above. Table 1 shows the results of the algorithm quantifying the geometric information content for the polygons shown in Fig. 2.

A drawback of the *convex hull* function is its inability to deal with either curvature or protrusions into the convex regions as defined by the hull. Such an inability is also shown in Fig. 2, polygon D. To help minimize the effect of this drawback, an additional step is introduced to this algorithm. The topology is rotated through a series of orientations. At each orientation the geometric information content is quantified using the method described. Some orientations allow the *convex hull* function to better articulate the empty spaces in the topology. Hence by taking the maximum of the set of information content in these orientations a more accurate quantification of the geometric information content in the topology is obtained.

When quantifying the information content due to the microstructure, it is not necessary to evaluate the orientation of every element in a topology. In general, the orientation of elements in the same sections of the topology tends to be similar. Therefore, the number of unique microstructures will often be less then the number of elements in the design domain. This grouping of similar orientations can be seen in Fig. 3. In this paper, similar

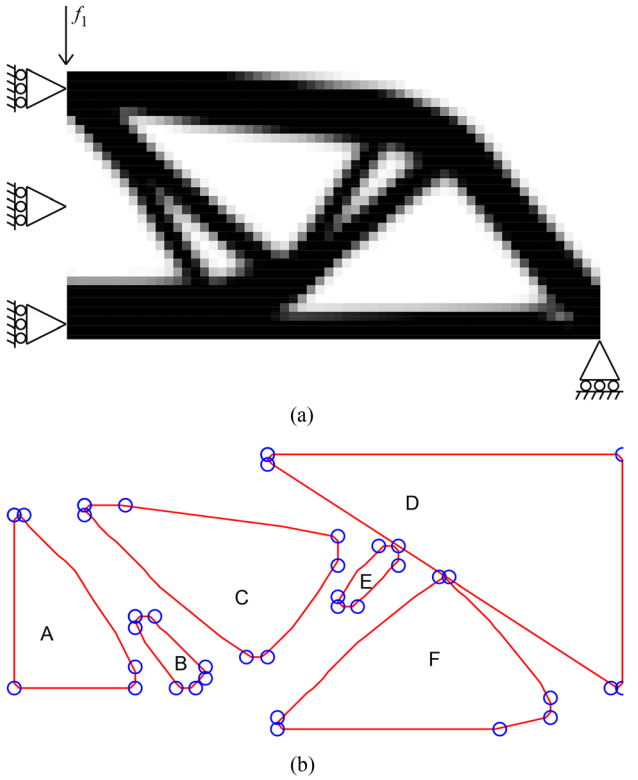

Fig. 2 Representation of how method describes voids. (*a*) Benchmark A. This is the solution to the topology optimization problem without attempting to add information content. This will be used for comparison to other isotropic examples. $\bar{C}_A = 100$ and $\bar{K}_A = 100$. (*b*) Convex hull representation of voids in Fig. 2(*a*)

Table 1 Information content

Method	Information
Algorithm	39
A	6
B	4
C	8
D	4
E	8
F	6
Total Hand Calc.	36

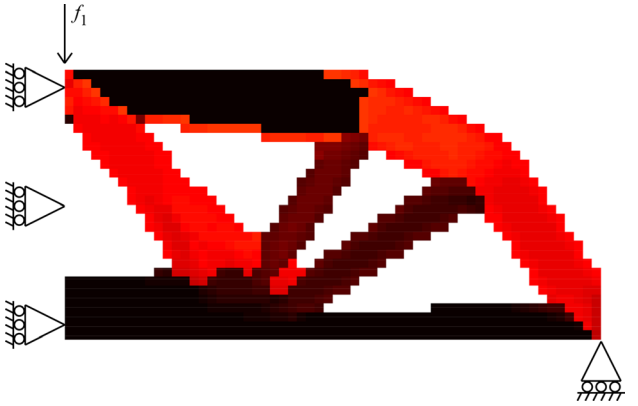

Fig. 3 An example of using different microstructure orientations in a topology. Each unique orientation adds 1 piece of information content. In this example information content (K) has been increased by 7.

orientations have been defined to be orientations that are within 10 deg of each other. The information content due to the microstructure is equal to the amount of unique microstructure groups in a topology.

2.3 How Information Content is Increased. Increasing the information content in a topology has been accomplished through increasing the geometric complexity and by allowing the microstructure orientation of each element to change. Each is now discussed.

2.3.1 Geometric Complexity. The more geometric complexity in a topology, the greater the amount of information content (K). Hence, maximizing geometric complexity becomes an objective. Under a topology optimization framework, geometric complexity can only be influenced by addition or subtraction of material within the design domain.

The redistribution of material in regions where local compliance is the highest is already incorporated into the SIMP method of topology optimization. However, in the code developed by Sigmund [21], there are no variables to directly control the geometric complexity of a topology. Therefore we have developed algorithms to work in conjunction with Sigmund's code to add geometric complexity.

In this paper, complicating the geometry has been accomplished by placing groups of elements in the design domain that are constrained to have zero material volume (i.e., constrained to be void regions). Creating these voids forces, the topology optimization routine to navigate around them. This often results in more complex geometry. Although this approach adds complexity to the geometry inadvertently it has been the most effective and simple of the methods tested. Figure 4(*a*) shows an example of voids being placed in the design domain and Fig. 4(*b*) shows the resulting topology after being optimized.

Using the original topology optimization result in Fig. 2(*a*) as a comparison, the topology in Fig. 4(*b*) has a 134% increase in K with a 25% increase in C. Thus adding voids to the design domain drastically increases the information content in a resulting topology. A drawback to this method is that it decreases the size of the design domain, ensuring that the average elemental compliance (C) will always be greater. This negative effect is counteracted by optimizing the microstructure orientation with the objective of minimizing C.

2.3.2 Microstructure Orientation. In this paper, the elements within the design domain are given microstructures that have anisotropic material properties. We have developed an algorithm to find the optimal orientation of each elements microstructure to reduce the average elemental compliance (C) in a topology. This simultaneously optimizes both of the optimization problem objectives. In Fig. 5, example results of this algorithm are shown. The C in Fig. 5(*b*) is 22% less than that of the uniformly oriented example in Fig. 5(*a*) and K has increased by 15%.

As previously stated, using the method of adding voids to the design domain to increase K will also negatively increase C for isotropic materials. Thus, the performance of the topology in Fig. 4(*b*) can easily be replicated with a different, less-complex geometry and the same volume fraction. This allows the clever engineer to make a simpler, better-performing product. Optimizing microstructure orientation resolves this issue as shown in Fig. 5. Note that even if the topology in Fig. 5(*b*) was created using the method of adding voids to the design domain, it would still have a lower C than the topology in Fig. 5(*a*). Thus, the greatest barrier to reverse engineering can be produced by combining both strategies: increasing geometric complexity and finding optimal microstructure orientation.

2.4 Solving the Optimization Problem. In this section, we describe the algorithms that have been developed to solve the optimization problem. These algorithms (i) find the optimal size and location of a given number of voids within the design domain to maximize geometric information content, and (ii) find the optimal microstructure orientation of each element to minimize the average elemental compliance in a topology. Each is discussed in the subsections below. These algorithms work in conjunction with Sigmund's topology optimization code [21] which already incorporates the optimization problem objective of minimizing the average elemental compliance.

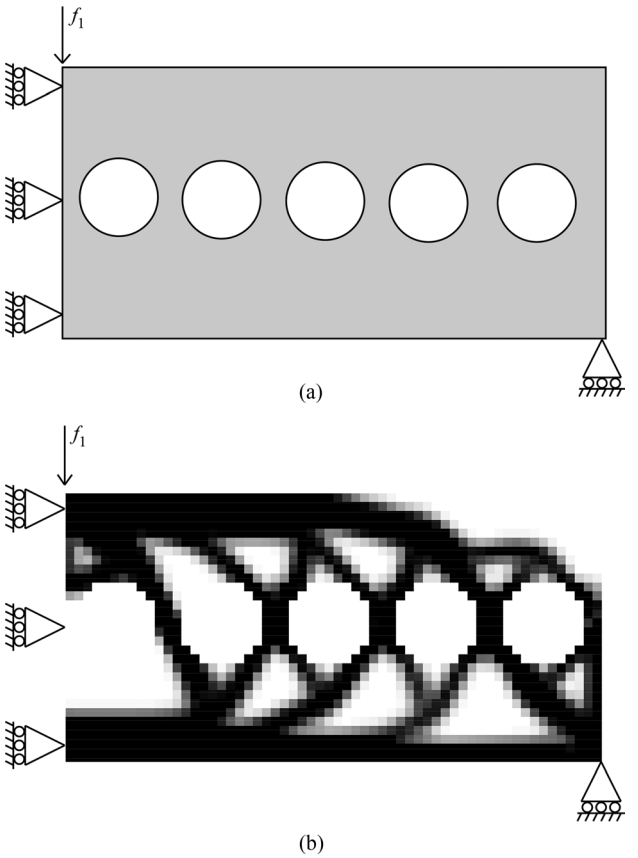

Fig. 4 Use of voids to increase information content. (*a*) Design domain with 5 equally spaced voids in an attempt to complicate the geometry (*b*) Resulting topology using the design domain in Fig. 4(*a*). $\bar{C}_A = 125$ and $\bar{K}_A = 234$. Where $\bar{C}_A = (C/C_A * 100)$ and $\bar{K}_A = (K/K_A * 100)$. C and K are evaluated from this topology, and C_A and K_A represent the C and K of the benchmark topology in Fig. 2(*a*).

The optimization problem is solved when the information content in the geometry and the microstructure has been increased by the algorithms described below. Therefore, the placement of the voids in the final design will be such that all the objectives in the optimization problem are minimized.

2.4.1 Optimum Void Location and Size. It has been determined that constraining groups of elements in the design domain to have no material volume (voids) often increases the geometric information content in a topology. Therefore, to maximize the information content for a certain number of voids, we have created an algorithm to find the location and size of the voids. The algorithm has not been designed with the number of voids as a computer manipulated design variable. Instead, it is a designer defined parameter chosen before the algorithm starts and is not changed during the execution of the algorithm. Any number of voids can be chosen by the designer with this guideline in mind; more voids generally produce a more geometrically complex topology, while at the same time increasing the time required to converge on an optimal topology. This algorithm begins by evenly spacing the circular voids in the design domain. The topology optimization is

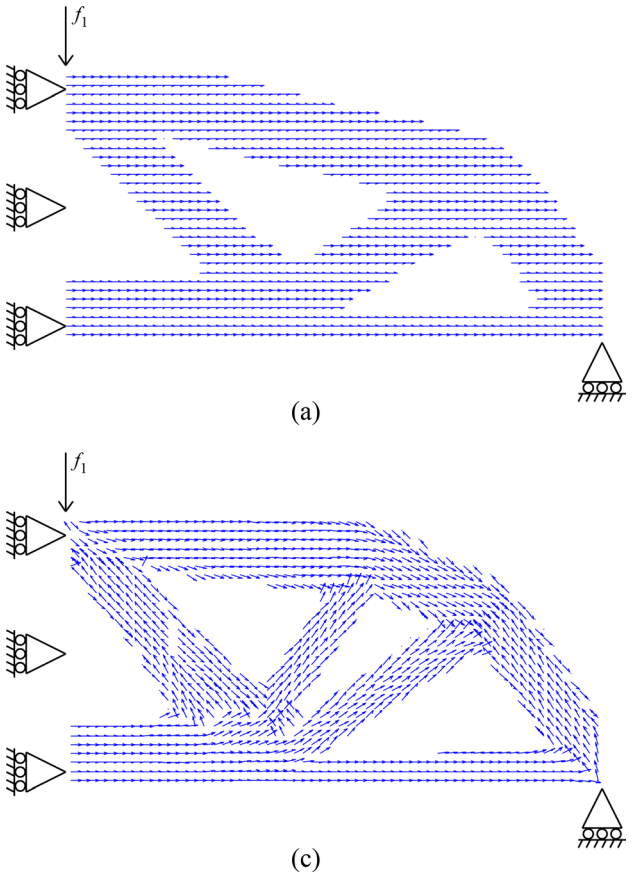

Fig. 5 Result of individually orienting the microstructure at each element. (*a*) Benchmark B. A topology optimization using a uniformly oriented anisotropic material. $\bar{C}_B = 100$ and $\bar{K}_B = 100$. Examples using an anisotropic material will be compared to this benchmark. (*b*) A topology optimization result using an anisotropic material that is optimally oriented at each element. $\bar{C}_B = 78$ and $\bar{K}_B = 115$

then solved and the information content (K) is evaluated. At this point, one void is allowed to randomly change its vertical position, horizontal position, and radius within the design domain. The random changes are determined by normally distributed random numbers, furthermore the changes are constrained to always lie within the design domain. The topology optimization is again solved and the information content for the new topology is found. This continues until (i) the information content is greater in the new topology or (ii) a specified maximum iteration is reached. The algorithm then moves to the next void and repeats the process. It continues to iterate through all the voids until it completes a cycle without finding a new topology with greater information content (K), thus finding an optimum for the specified number of voids. A flow chart of this algorithm can be seen in Fig. 6, and the results of this method can be seen in Fig. 7. The (K) in this example is 192% of that in Fig. 2(*a*).

2.4.2 Optimal Microstructure Orientation. As previously explained, each element in the design domain has a microstructure that yields anisotropic material properties. Figure 8 highlights one of these elements. For the results in Sec. 2, the anisotropic material properties are such that the Young's Modulus in the 1 direction is twice that of the Young's Modulus in the 2 direction. Figure 8 also illustrates how the variable Θ is able to change the orientation of the microstructure and therefore control the material properties of each element. For Θ to accomplish this within the topology optimization it defines a transformation matrix used to transform the anisotropic constitutive matrix for each element [31].

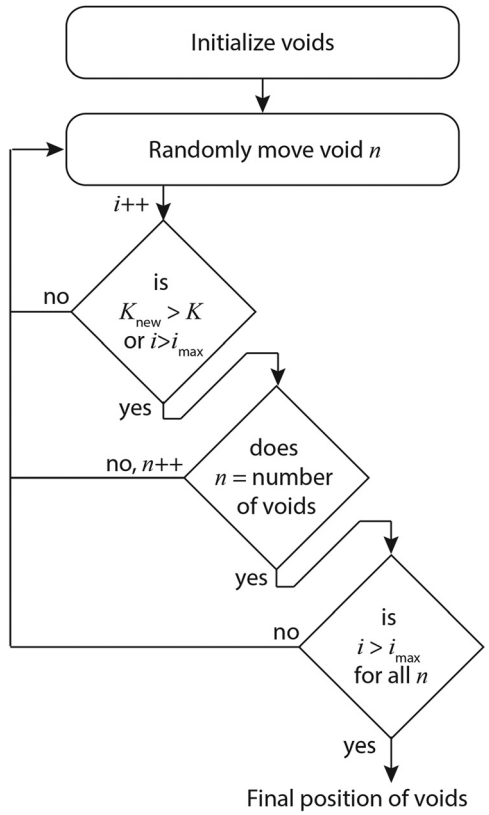

Fig. 6 Flow chart summarizing the algorithm that finds the optimal placement of the voids

There exists a Θ for each element that will minimize the compliance within that element. The algorithm developed to find the microstructure orientation that minimizes C for a topology solves for Θ in each element. The optimal value of Θ has been found to be equal to the orientation of the highest principal stress. Therefore, it is necessary to identify the orientation of the highest principal stress in each element. To accomplish this, the finite element routine used in Sigmund's code was modified to calculate the principal stresses. The maximum of the two principal stresses was then determined and its orientation calculated.

3 Examples

This section demonstrates how the methods introduced in this paper can be used for the design of a novel electrical contact for a

Fig. 7 Resulting topology from using four voids and allowing them to move their location and size to find an optimum solution. $\bar{C}_A = 134$ and $\bar{K}_A = 192$.

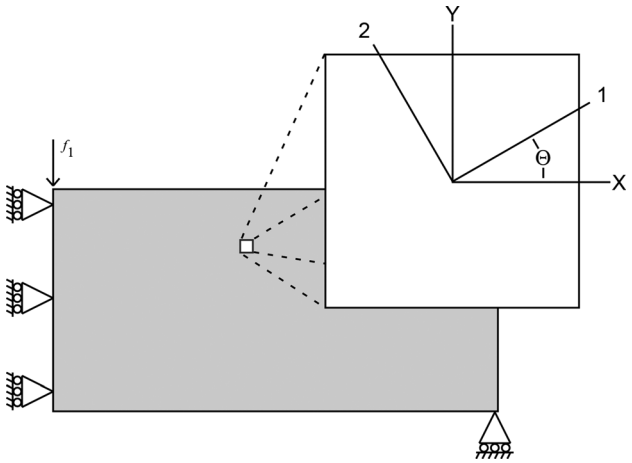

Fig. 8 Design domain with one element highlighted. This elements microstructure orientation is determined by the value of Θ.

consumer electronics product. Many electrical contacts are manufactured through progressive die forming. As such, many contacts have large width to height ratios. Given the market demand for miniaturization of electronics, some electrical contact manufactures are beginning to explore the benefits of contacts with very low width to height ratios. This section describes such a contact and shows that topology optimization can be used to identify a contact topology that could be fabricated from a planar sheet of copper and require no die forming, thus simplifying the manufacturing to a blanking process. Validating the financial benefit of this simplification is not the focus of this paper.

To function properly from an electrical point of view, electrical contacts require a certain contact normal force for a given deflection. The design requirements for this example are that the contact must have a deflection between 0.35 mm and 1 mm for a contact normal force of 1 N. Also for this example, designs with a deflection closer to 0.35 mm are preferred. In this design, a cube textured copper material is used. This material has been chosen because of the large variation of its material properties associated with its different microstructure orientations [32].

The design domain with the boundary conditions and loads are defined as shown in Fig. 9. This design domain has a horizontal dimension of 25 mm and a vertical dimension of 10 mm. The downward force is 1 N, and the horizontal force is 0.5 N (simulating the maximum horizontal force seen by the electrical contact during connection). The electrical contact is fixed on the lower half of its left side in all degrees of freedom. The design domain for these examples has been discretized into square elements with side lengths of 0.25 mm. Executing the topology optimization routine based on this design domain results in the topology shown in Fig. 10. Note that for this case, the number of unique microstructures is constrained to be 1. This first design (case 1) of the electrical contact will be used as a benchmark to the remaining examples.

Fig. 9 Design domain for the novel electrical contact

Fig. 10 Case 1:(Benchmark C) Uniformly oriented Topology with no forced voids. $\bar{C}_C = 100$ and $\bar{K}_C = 100$.

Fig. 11 Case 2: Uniformly oriented topology with 4 forced voids that have been optimally located and sized. $\bar{C}_C = 109.5$ and $\bar{K}_C = 192$.

The next three designs show the results of the algorithms developed in this paper working in conjunction with the topology optimization routine to maximize K and minimize C. Case 2 (shown in Fig. 11) is a design of the electrical contact after 4 voids have been optimally located and sized within the design domain using the method described in Sec. 2.4.1. Within the algorithm, the voids random changes in location and size are determined from a normal distribution with a mean of 0 and a standard deviation of 5% of the design domain. For case 2, one unique microstructure is allowed. The voids in case 4 are created the same way. Case 3 (shown in Fig. 12) is a design of the electrical contact where the microstructure of each element in the design domain has been optimally oriented. Case 4 (shown in Fig. 13) is a design where 4 voids have been optimally located and sized within the design domain (as described in case 2), and the microstructure of each element in the design domain has been optimally oriented.

In Table 2, a comparison of information content and the deflection of the electrical contact can be seen for each case.

Case 2 (compared to the benchmark design) has an increased information content (K), but the deflection has undesirably

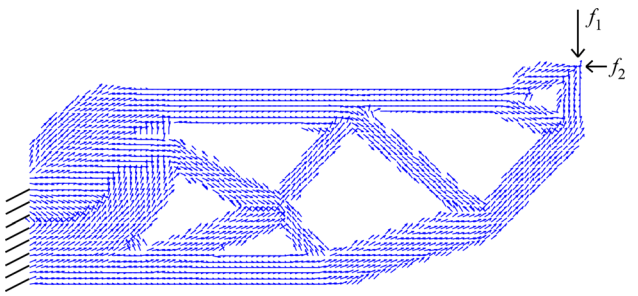

Fig. 12 Case 3: Optimally oriented topology with no forced voids. $\bar{C}_C = 71$ and $\bar{K}_C = 132$

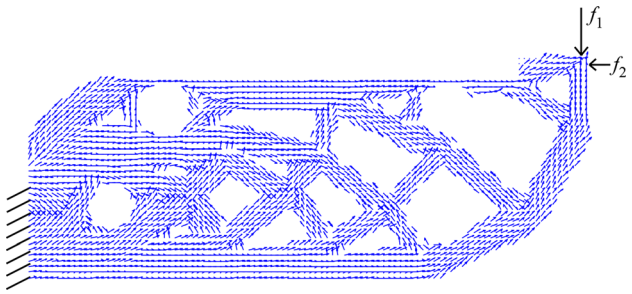

Fig. 13 Case 4: Optimally oriented topology with 4 forced voids that have been optimally located and sized. $\bar{C}_C = 79$ and $\bar{K}_C = 250$.

Table 2 Comparison of information content (K) and Deflection in the different cases

Example	Info. content	deflection (mm)
Case 1 (benchmark)	44	0.53
Case 2	77	0.58
Case 3	58	0.375
Case 4	98	0.42

increased. Although this design would be more difficult to reverse engineer, a clever engineer would be able to create a simpler beam using less material that had the same deflection; resulting in a better, less-expensive product. Although this risk is present when using the design in case 2, the time to reverse engineer the product has been increased.

Case 3 has the lowest deflection (which is desirable) out of the 4 designs. Also, compared to the benchmark the K has increased. This shows that by manipulating the microstructure, a designer is able to increase the time to reverse engineering a product while simultaneously improving the product's performance. This design has the absolute lowest possible defection for the given design domain. However, the information content, K, can still be drastically increased.

Case 4 has the greatest amount of K and a desirably low deflection. Even though its deflection is not as low as the deflection in case 3, it is lower then the deflection found in the benchmark design. Thus, it has a better performance than the benchmark design and a much higher information content. Therefore, case 3 and case 4 are able to increase the time to reverse engineering a product without giving up the desirable structural characteristic of compliance. Although case 4 has a slight increase in deflection over case 3, it has a drastic increase in K, potentially making it the superior design. A CAD model of this design can be seen in Fig. 14

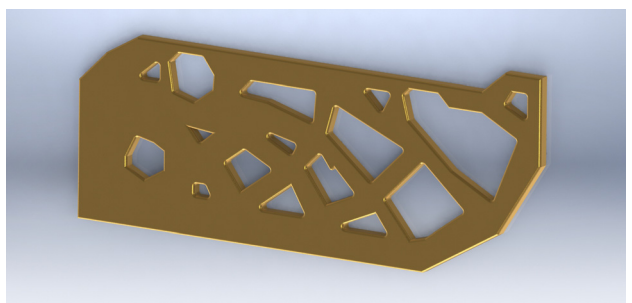

Fig. 14 3D Model of the design in case 4

4 Conclusion

This paper has shown that the tool of topology optimization can be used to identify topologies that are both time-consuming to reverse engineer and structurally desirable. The new aspects of this paper include algorithms that enable topology optimization to be used in this way. Specifically, an algorithm is presented that automatically evaluates the information content of any two-dimensional topology. This evaluation allows an additional objective, the maximization of information content, to be added to traditional topology optimization objectives. To make the inclusion of this objective more meaningful, microstructure sensitive design is also folded into the process by allowing individual topology elements to be optimally oriented. Various test cases are performed in the paper. Using isotropic materials and maximizing information content results in an undesirable increase in structural compliance. When using anisotropic materials, minimizing structural compliance and maximizing information content can occur desirably without significant compromise. This comes from increasing the information content held in both the geometry and microstructure of a topology. An electrical contact for a consumer product is also examined. Because the topology optimization is able to examine numerous complicated contact designs in search of one that would out perform traditional isotropic progressive-die formed contacts, a contact is found that competitors would want to reverse engineer, yet have significant difficulty doing so.

Acknowledgment

The authors would like to acknowledge Kevin C. Francis, who helped develop the code that evaluates the information content in a topology.

Nomenclature

C = average elemental compliance
f = force vector
J = optimization variable
k = stiffness matrix
K = information content
K_g = information content held in the geometry
K_m = information content held in the microstructure
K_0 = initial information content
T = time to reverse engineer a product
u = displacement vector
V_x = material volume
V_0 = design domain volume
x = vector of element densities
$x_{\min}$ = vector of minimum element densities
v = material volume fraction (V_x/V_0)
Θ = microstructure orientation angle
$\overline{()}$ = normalized value of $()$

References

[1] Samuelson, P., and Scotchmer, S., 2001, "Law and Economics of Reverse Engineering," Yale LJ, **111**, p. 1575.
[2] McLoughlin, I., 2008, "Secure Embeddeed Systems: The Threat Of Reverse Engineering," ICPADS'08. 14th IEEE International Conference on Parallel and Distributed Systems, pp. 729–736.
[3] Naumovich, G., and Memon, N., 2003, "Preventing Piracy, Reverse Engineering, and Tampering," Computer, **36**(7), pp. 64–71.
[4] Grand, J., 2004, "Practical Secure Hardware Design for Embedded Systems," Proceedings of the 2004 Embedded Systems Conference.
[5] Campbell, R. J., and Flynn, P. J., 2001, "A Survey of Free-Form Object Representation and Recognition Techniques," Comput. Vis. Image Underst., **81**(2), pp. 166–210.
[6] Schuh, G., Haag, C., and Kreysa, J., 2011, "Triz-Based Technology Know-How Protection-How to Find Protective Mechanisms Against Product Piracy With," Procedia Eng., **9**(0), pp. 611–619.
[7] Curtis, S., Harston, S., and Mattson, C., 2011, "The Fundamentals of Barriers to Reverse Engineering and Their Implementation into Mechanical Components," Res. Eng. Des., pp. 1–17.
[8] Harston, S., Mattson, C., and Adams, B., 2010, "Metrics for Evaluating the Barrier and Time To Reverse Engineer a Product," ASME J. Mech. Des., **132**(4), p. 041009.

[9] Reed, R., and Defillipi, R., 1990, "Causal Ambiguity, Barriers to Imitation, and Sustainable Competitive Advantage," Acad. Manage. Rev.,**15**, pp. 88–102.
[10] Bendsoe, M. P., and Sigmund, O., 2004, *Topology Optimization: Theory, Methods and Applications*, Springer, New York.
[11] Sigmund, O. T. S., 1997, "Design of Materials With Extreme Thermal Expansion Using a Three-Phase Topology Optimization Method," J. Mech. Phys. Solids **45**, pp. 1037–1067.
[12] Zhou, H., and Killekar, P. P., 2011, "The Modified Quadrilateral Discretization Model for the Topology Optimization of Compliant Mechanisms," ASME J. Mech. Des., **133**(11), p. 111007.
[13] Kota, S., Joo, J., Li, Z., Rodgers, S., and Sniegowski, J., 2001, "Design of Compliant Mechanisms: Applications to Mems," Analog Integr. Circuits Signal Process., **29**, pp. 7–15.
[14] Lee, S., and Tovar, A., 2013, "Topology Optimization of Piezoelectric Energy Harvesting Skin Using Hybrid Cellular Automata," ASME J. Mech. Des., **135**(3), p. 031001.
[15] Nomura, T., Nishiwaki, T., Nishiwaki, S., Sato, K., and Hirayama, K., 2009, "Topology Optimization for the Design of periodic Microstructures Composed of Electromagnetic Materials," Finite Elem. Anal. Design, **45**, pp. 210–226.
[16] Rakshit, S., and Ananthasuresh, G., 2008, "Simultaneous Material Selection and Geometry Design of Statically Determinate Trusses Using Continuous Optimization," Struct. Multidiscip. Optim., **35**, pp. 55–68.
[17] Li, Q., Steven, G. P., Querin, O. M., and Xie, Y., 1999, "Shape and Topology Design For Heat Conduction by Evolutionary Structural Optimization," Int. J. Heat Mass Transfer, **42**(17), pp. 3361–3371.
[18] Torquato, S., Hyun, S., and Donev, A., 2002, "Multifunctional Composites: Optimizing Microstructures For Simultaneous Transport of Heat and Electricity," Phys. Rev. Lett., **89**, p. 266601.
[19] Bendsoe, M., 1989, "Optimal Shape Design as a Material Distribution Problem," Struct. Optim., **1**, pp. 193–202.
[20] Rozvany, G., 2009, "A Critical Review of Established Methods of Structural Topology Optimization," Struct. Multidiscip. Optim., **37**, pp. 217–237.
[21] Sigmund, O., 2001, "A 99 Line Topology Optimization Code Written In Matlab," Struct. Multidiscip. Optim., **21**, pp. 120–127.
[22] Challis, V., 2010, "A Discrete Level-Set Topology Optimization Code Written In Matlab," Struct. Multidiscip. Optim., **41**, pp. 453–464.
[23] Yamada, T., Izui, K., and Nishiwaki, S., 2011, "A Level Set-Based Topology Optimization Method for Maximizing Thermal Diffusivity in Problems Including Design-Dependent Effects," ASME J. Mech. Des.,**133**(3), p. 031011.
[24] Adams, B. L., Kalidindi, S. R., Fullwood, D. T., and Niezgoda, S. R., 2010, "Microstructure Sensitive Design for Performance Optimization," Prog. Mater. Sci., **55**(6), pp. 477–562.
[25] Harston, S., Mattson, C., and Adams, B., 2010, "Capitalizing on Heterogeneity and Anisotropy to Design Desirable Hardware That is Difficult to Reverse Engineer," ASME J. Mech. Des., **132**(8), p. 081001.
[26] Messac, A., and Mattson, C., 2002, "Generating Well-Distributed Sets of Pareto Points For Engineering Design Using Physical Programming," Optim. Eng., **3**, pp. 431–450.
[27] Balling, R., 1999, "Design by Shopping: A New Paradigm?," Proceedings of the Third World Congress of Structural and Multidisciplinary Optimization (WCSMO-3), vol. 1, pp. 295–297.
[28] Zhang, X., Xie, J., Xie, H., and Li, L., 2012, "Experimental Investigation on Various Tool Path Strategies Influencing Surface Quality and Form Accuracy of Cnc Milled Complex Freeform Surface," Int. J. Adv. Manuf. Technol., **59**(5-8), pp. 647–654.
[29] Bi, Z., and Wang, L., 2010, "Advances in 3d Data Acquisition and Processing for Industrial Applications," Rob. Comput.-Integr. Manufact., **26**(5), pp. 403–413.
[30] Mohaghegh, K., Sadeghi, M., and Abdullah, A., 2007, "Reverse Engineering of Turbine Blades Based on Design Intent," Int. J. Adv. Manuf. Technol., **32**(9-10), pp. 1009–1020.
[31] Li, S., and Atluri, S., 2008, "The Mlpg Mixed Collocation Method for Material Orientation and Topology Optimization of Anisotropic Solids and Structures," Comput. Model. Eng. Sci., **30**(1), pp. 37–56.
[32] Takahashi, R., Prasai, D., Adams, B. L., and Mattson, C. A., 2012, "Hybrid Bishop-Hill Model for Elastic-Yield Limited Design With Non-Orthorhombic Polycrystalline Metals," ASME J. Eng. Mater. Technol., **134**(1), p. 011003.